Optical guiding in a sheet-beam free-electron laser

Amnon Fruchtman
Department of Nuclear Physics, Weizmann Institute of Science, 76 100 Rehovot, Israel
(Received 17 September 1987)

The influence of electron density gradients on optical guiding in free-electron lasers (FEL's) is considered. We study a model problem of a FEL which employs a sheet electron beam in the absence of a cavity or a waveguide. We calculate the gain and the rate of optical guiding by solving for the eigenvalues and the actual eigenmodes of the system. Similar to what has been found by Moore for a cylindrical beam [Nucl. Instrum. Methods **A239**, 19 (1985)], we find that two parameters characterize the interaction: a coupling parameter and a detuning parameter. We solve the problem for two density profiles, a uniform density profile and a triangular-shaped density profile. For large and small values of the coupling parameter we obtain the results analytically. For intermediate values of the coupling parameter we obtain numerical results. When the coupling parameter is small, diffraction is large. The gain and the wave profile are then similar for the two density profiles. When the coupling parameter is large, optical guiding is large. The gain for the triangular-shaped beam is then larger by $2^{1/3}$ than the gain for the uniform beam. When the coupling parameter is large, the wave profile for the uniform density beam converges to a certain profile confined to the beam volume. For the triangular-shaped beam the wave profile becomes more and more concentrated near the midplane of the sheet beam. For the solution of the problem we derive an energy integral that determines the domain in the complex plane where nonreal eigenvalues are allowed. We also show the existence of an accumulation point of nonreal eigenvalues in certain cases.

I. INTRODUCTION

Optical guiding in free-electron lasers (FEL's) (Ref. 1) has recently become a subject of extensive theoretical[2–5] and experimental[6] study. The guiding of the amplified wave by the electron beam cancels the need for a cavity or a waveguide. It also increases the filling factor, the ratio between the cross sections of the electron beam and the wave beam, and thus strengthens the interaction. In this paper we are interested in optical guiding in the linear growth regime of the FEL. We find the conditions under which growing eigenmodes of the system are confined to the volume of the electron beam.

We adopt the approach of reducing the Maxwell and the cold-fluid equations to a two-point boundary value problem with an eigenvalue. The solutions for the wave fields are required to be bounded at infinity. The eigenvalues determine the growth rate of the FEL instability, and the eigenfunctions describe the transverse profile of the wave. The wave fields are described without the use of vacuum modes or of other systems of orthogonal functions. Instead, we solve for the actual eigenmodes of the system. A similar approach was taken by Moore[3] who a analyzed a FEL with a cylindrical beam of uniform density.

We examine a FEL which employs a rectangular, or sheet, electron beam in a planar wiggler. Experiments with such a sheet-beam FEL in a planar wiggler have recently been reported.[7] The electron beam propagates in the z direction and is thin in the y direction, the direction of both the wiggler field and the transverse gradient of the wiggler field. The electron beam is much thicker in the x direction, which is possible practically because the planar wiggler has weak x dependence. The use of such a sheet electron beam enables one to increase the current by increasing the beam cross section through making the beam wide in the x direction. This is in contrast to increasing the current by increasing the beam density which, for high-current beams, is difficult because of the generation of strong repulsive self-fields. Since the wiggler field depends only weakly on x, the relatively wide-x dimension of the beam does not induce inhomogeneities which would be destructive to the resonance conditions of the FEL. We assume the sheet beam to be infinite in the x dimension and finite in the y dimension. We assume further that all the quantities are x independent and that all the transverse dependence is on y only. We write the Maxwell and the cold-fluid equations which are y and z dependent. We then simplify the equations near the FEL resonance to be y dependent only. The governing equation which is thus obtained, is a second-order ordinary differential equation with an eigenvalue. The growth rate of the FEL instability is given by the imaginary part of the eigenvalue. Similarly to Moore we select the solution which vanishes at infinity and which satisfies certain continuity conditions across the beam boundary.

We calculate the gain and the rate of optical guiding for two density profiles. The first is a step profile, where the beam is uniform but finite in the y direction. The second profile is triangular shaped, where the density falls linearly in y from its maximal value in the midplane of the sheet to zero on the beam boundary.

We find that in addition to the beam radial density profile, there are two characteristic parameters: a cou-

pling parameter, which is a combination of the wiggler strength and the electron current, and a detuning parameter. We solve the problem analytically for large and small values of the coupling parameter for the two density profiles. For intermediate values of this parameter we find the results numerically.

When the coupling parameter is large, optical guiding is dominant for both density profiles. For the uniform beam the gain scales as in the one-dimensional (1D) theory, similar to the gain for the cylindrical beam.[3] For the triangular-shaped beam the gain is larger by a factor of $2^{1/3}$ than for the uniform beam, when both beams have the same current and the same thickness. In this case of strong optical guiding, the wave is confined to the beam volume for the uniform beam and to the midplane for the triangular-shaped beam. The opposite case of small coupling coefficient is the case of large diffraction. Here the wave extends well beyond the beam boundaries and for the fundamental mode is nearly constant across the beam. The gain is the same for both density profiles. Contrary to the case of a cylindrical beam,[3] the normalized gain does not diverge when the coupling parameter goes to zero but converges to a constant. That constant is the same for both density profiles.

We are interested mainly in the most unstable mode. However, we also show the existence of an accumulation point of infinite unstable modes. We assume that the electron beam is thin enough so that we can ignore the transverse dependence of the wiggler field. We also only consider a tenuous beam and neglect the static self-fields of the electrons. (This is in contrast to our recent analysis of the FEL interaction where the wiggler transverse gradients and beam static self-fields were not negligible and in fact played a major role.[8–10])

In Sec. II we derive the governing equation. In Sec. III we formulate an energy integral which determines the domain in the complex plane where nonreal eigenvalues are allowed. In Sec. IV we solve the equation for the constant density electron beam and in Sec. V for the triangular-shaped electron beam. We give numerical examples and conclude in Sec. VI.

II. THE GOVERNING EQUATION

We describe the electron-beam dynamics by the cold-fluid equations. These are the continuity equation

$$\frac{1}{c}\frac{\partial}{\partial t}(\gamma H)+\nabla\cdot(\mathbf{P}H)=0 , \tag{1}$$

and the momentum equation

$$\frac{\gamma}{c}\frac{\partial \mathbf{P}}{\partial t}+\mathbf{P}\cdot\nabla\mathbf{P}=-\gamma\mathbf{E}-\mathbf{P}\times\mathbf{B} . \tag{2}$$

Here $\mathbf{P}$ is the normalized momentum (the momentum divided by mc), γ is $(1+\mathbf{P}\cdot\mathbf{P})^{1/2}$, H is the normalized density [the density multiplied by $4\pi e^2/(mc^2\gamma)$], e and m are the electron charge and mass, c is the velocity of light in vacuum, and $\mathbf{E}$ and $\mathbf{B}$ are the normalized electric and magnetic fields [the fields multiplied by $e/(mc^2)$].

The electron beam we consider propagates along a planar magnetic wiggler field of the approximated form

$$\mathbf{B}_0=\hat{\mathbf{e}}_y B_w \sin(k_0 z) . \tag{3}$$

The electron beam is assumed to be infinitely long in the z direction, and its transverse cross section is assumed to be rectangular. We make the further assumption that the beam is infinitely long in the x direction since we assume that the beam width in that direction is much larger than its width in the y direction. We require

$$k_0 a \ll 1 , \tag{4}$$

where $2a$ is the thickness of the beam in the y direction. Inequality (4) is necessary (though not always sufficient) for the validity of form (3) for the magnetic wiggler. The governing equations of the FEL interaction have been derived many times before. We rederive them in a form suited to our purpose. We limit ourselves to solutions which do not depend on x.

In order to perform a linear stability analysis we write each quantity as a sum of zeroth-order time-independent terms and first-order time-dependent terms of the form

$$H(y,z,t)=h(y,z)+\mathrm{Re}[\delta h(y,z)e^{-i\omega ct}] , \tag{5a}$$

$$\mathbf{P}(y,z,t)=\mathbf{p}(y,z)+\mathrm{Re}[\delta\mathbf{p}(y,z)e^{-i\omega ct}] , \tag{5b}$$

$$\gamma(y,z,t)=\Gamma(y,z)+\mathrm{Re}[\delta\gamma(y,z)e^{-i\omega ct}] , \tag{5c}$$

$$\mathbf{B}(y,z,t)=\mathbf{B}_0(z)+\mathrm{Re}[\delta\mathbf{B}(y,z)e^{-i\omega ct}] , \tag{5d}$$

$$\mathbf{E}(y,z,t)=\mathrm{Re}[\delta\mathbf{E}(y,z)e^{-i\omega ct}] . \tag{5e}$$

We neglect static self-fields of the beam. Time-independent solutions of Eqs. (1) and (2), in the presence of the field (3), are

$$\Gamma(y,z)=\Gamma=\text{const} , \tag{6a}$$

$$p_x(z)=-\frac{B_w}{k_0}\cos(k_0 z) , \tag{6b}$$

$$p_y=0 , \tag{6c}$$

$$p_z^2(z)=\Gamma^2-1-\frac{B_w^2}{k_0^2}\cos^2(k_0 z) , \tag{6d}$$

$$h(y,z)=h(y,0)p_z(0)/p_z(z) . \tag{6e}$$

Usually B_w^2/k_0^2 is much smaller than (Γ^2-1) and we may approximate

$$p_z(z)=(\Gamma^2-1)^{1/2}\left[1-\frac{1}{2(\Gamma^2-1)}\frac{B_w^2}{k_0^2}\cos^2 k_0 z\right] . \tag{7}$$

We are interested in the fundamental resonance and may further approximate

$$p_z(z)=(\Gamma^2-1)^{1/2} \tag{8}$$

and

$$h(y,z)\cong h(y,0) . \tag{9}$$

Having completed the solution for the steady-state flow, we turn now to the first-order terms. Since p_y is zero and

since $\mathbf{p}$ does not depend on y, the linearized momentum equation is

$$-iw\Gamma\,\delta\mathbf{p}+p_z\frac{\partial\delta\mathbf{p}}{\partial z}=-\Gamma\,\delta\mathbf{E}-\delta\mathbf{p}\times\mathbf{B}_0-\mathbf{p}\times\delta\mathbf{B}\ . \tag{10}$$

The quantities in this equation depend on both y and z. However, because the derivative is with respect to z only, as it is in the 1D approximation, we continue the analysis in a somewhat condensed form. Because of the periodicity of the steady-state flow, each perturbed quantity is written as

$$\delta\mathbf{f}(y,z)=e^{ikz}\sum_{n=-\infty}^{\infty}\delta\mathbf{f}_n(y)e^{ink_0z}\ . \tag{11}$$

We are interested in k close to ω and assume that the largest Fourier components of the wave fields are $\delta\mathbf{E}_0$ and $\delta\mathbf{B}_0$. If, in addition,

$$\omega\Gamma-(k+k_0)p_z\cong 0\ , \tag{12}$$

one of the Fourier components of the longitudinal momentum, $\delta p_{z,1}$, becomes large. The transverse components $\delta p_{x,1}$ and $\delta p_{y,1}$ are not resonant since the sources in the components of the momentum equation which determine them are small. Thus approximately,

$$i(-\omega\Gamma+kp_z)\delta p_{x,0}=-\Gamma_0\delta E_{x,0}+p_z\delta B_{y,0}\ , \tag{13}$$

$$i[-\omega\Gamma+(k+k_0)p_z]\delta p_{z,1}=\frac{B_w}{2k_0}\delta B_{y,0}-\frac{B_w}{2i}\delta p_{x,0}\ , \tag{14}$$

which yield for $\delta p_{z,1}$ [by using Eq. (12)]

$$\delta p_{z,1}=-\frac{iB_w\Gamma}{2k_0p_z}\frac{\delta E_{x,0}}{[-\omega\Gamma+(k+k_0)p_z]}\ . \tag{15}$$

The perturbed continuity equation is

$$-i\omega\Gamma\delta h-i\omega h\delta\gamma+p_z\frac{\partial\delta h}{\partial z}+h\frac{\partial\delta p_z}{\partial z}+h\frac{\partial\delta p_y}{\partial y}+\delta p_y\frac{\partial h}{\partial y}=0\ . \tag{16}$$

Since δp_y is not resonant and is much smaller than δp_z, and since

$$\Gamma\delta\gamma\cong p_z\delta p_z\ , \tag{17}$$

the perturbed density is

$$\delta h_1=-\frac{2hk_0p_z\delta p_{z,1}}{\Gamma[-\omega\Gamma+(k+k_0)p_z]}\ . \tag{18}$$

The perturbed current, the source in Maxwell's equations, is

$$\delta\mathbf{j}=-h\,\delta\mathbf{p}-\mathbf{p}\delta h\ . \tag{19}$$

To lowest order, this current is

$$\delta\mathbf{j}=-\hat{\mathbf{e}}_xp_x\delta h\ . \tag{20}$$

Substituting this expression into the Maxwell equation and using the fact that $\delta\mathbf{E}_0$ is dominant over the other wave Fourier components, we arrive at the following final form of the equations:

$$\frac{\partial^2\delta E_x}{\partial y^2}+(\omega^2-k^2)\delta E_x=\frac{h\omega B_w^2\delta E_x}{2k_0[-\omega\Gamma+(k+k_0)p_z]^2}\ . \tag{21}$$

We omitted the subscript zero in the notation for the zeroth Fourier component of the wave fields. One may note that the form of the source term, the right-hand side (RHS) of the equation, is similar to the form in the 1D theory. This occurs because the steady-state momentum does not have a y component and because the chosen steady state has no x dependence. A different geometry could produce a more complicated equation, where the transverse dependence of the steady state changes the form of the equation. near the FEL resonance both (ω^2-k^2) and $[-\omega\Gamma+(k+k_0)p_z]$ are small. We may then approximate

$$\omega^2-k^2=-2\omega(k-\omega)=-2\omega\nu\ , \tag{22a}$$

$$-\omega\frac{\Gamma}{p_z}+(k+k_0)=\nu+\xi=\nu+k_0+\omega\left[1-\frac{\Gamma}{p_z}\right]\ , \tag{22b}$$

where ν is the eigenvalue and ξ is a detuning (mismatch) parameter. We look for nonreal eigenvalues. Those with negative imaginary parts correspond to growing modes.

In Eq. (21) for δE_x the y dependence of the coefficients is only through the density h. We assume

$$h(y)=0,\quad |y|\geq a \tag{23}$$

multiply Eq. (21) by a^2, and write it in the following nondimensional form:

$$\frac{\partial^2\delta E_x}{\partial\bar{y}^2}+\phi^2\delta E_x-\alpha\bar{h}(\bar{y})\frac{\delta E_x}{(\phi^2-\mu)^2}=0\ . \tag{24}$$

The independent variable is

$$\bar{y}\equiv y/a\ , \tag{25}$$

and the normalized eigenvalue and mismatch parameter are

$$\phi^2=-2\omega\nu a^2\ , \tag{26a}$$

$$\mu=2\omega\xi a^2\ . \tag{26b}$$

We are now looking for a nonreal ϕ^2 with a positive imaginary part. The quantity α in Eq. (24) is defined as

$$\alpha=(Ja)(\omega a)^3\left[\frac{B_w}{k_0p_z}\right]^2(k_0a)\ , \tag{27}$$

and the normalized current J and density $\bar{h}$ are

$$J=\int_{-\infty}^{\infty}dy\,h(y)\ , \tag{28a}$$

$$\bar{h}(\bar{y})=2ah(y)/J\ . \tag{28b}$$

Equation (24) is equivalent to the equation derived by Moore[3] for the cylindrical geometry. We have adopted some of his notations.

Our purpose is to study the dependence of the solutions of Eq. (24) on the parameter α for two density profiles $\bar{h}(\bar{y})$. We examine the dependence of the gain, the imaginary part of ϕ^2, on this parameter. We also address the question of optical guiding, i.e., the extent to

which the wave beam is confined to the volume that the electron beam occupies. We derive scaling laws where possible and complement them with numerical calculations. We start by determining the domains in the complex ϕ^2 plane where nonreal eigenvalues are allowed. A similar energy integral was derived in Ref. 9.

III. DERIVATION OF AN ENERGY INTEGRAL

We multiply Eq. (24) by δE_x^* and integrate from $-\infty$ to ∞, assuming the integral exists. Integration by parts yields

$$-\int_{-\infty}^{\infty} d\bar{y} \left| \frac{d\delta E_x}{dy} \right|^2 + \int_{-\infty}^{\infty} d\bar{y} \, |\delta E_x|^2 \times \left[\phi^2 - \frac{\alpha \bar{h}}{(\phi^2-\mu)^2} \right] = 0 . \quad (29)$$

Taking the imaginary part of the equation and assuming $\mathrm{Im}\phi^2$ is not zero, we obtain

$$\int_{-\infty}^{\infty} d\bar{y} \, |\delta E_x|^2 \left[1 + 2\frac{\alpha \bar{h} \mathrm{Re}(\phi^2-\mu)}{|\phi^2-\mu|^4} \right] = 0 . \quad (30)$$

As in Rayleigh's inflection theorem[11] the term in the large parentheses has to take both positive and negative values. Since when $\bar{h}$ equals zero this term is positive, for some $\bar{y}$ the density $\bar{h}$ must be large enough to make the term negative. Possible nonreal eigenvalues are those which obey

$$1 + \frac{2\alpha h_+ \mathrm{Re}(\phi^2-\mu)}{|\phi^2-\mu|^4} < 0 , \quad (31a)$$

and

$$1 + \frac{2\alpha h_- \mathrm{Re}(\phi^2-\mu)}{|\phi^2-\mu|^4} > 0 , \quad (31b)$$

where h_+ and h_- are the maximal and minimal values of $\bar{h}$, respectively. If the wave extends beyond the volume that the beam occupies, h_- is simply zero, i.e., Eq. (32b) is trivially satisfied. If, however, there is a conductor at $\bar{y} = \pm 1$, and h_- does not equal zero, Eq. (32b) constitutes a constraint for the eigenvalue. Denoting

$$F_\pm \equiv (\alpha h_\pm)^{1/3} , \quad (32a)$$

we can easily show that the maximal possible imaginary part of ϕ^2 is

$$(\mathrm{Im}\phi^2)_{\max} = y_1 = \frac{\sqrt{3}}{2} F_+ \quad (32b)$$

when

$$\mathrm{Re}(\phi^2-\mu) = X_1 = -\frac{F_+}{2} . \quad (32c)$$

Also nonreal eigenvalues are possible if

$$X_2 < \mathrm{Re}(\phi^2-\mu) < 0 , \quad (33a)$$

where

$$X_2 \equiv -2^{1/3} F_+ . \quad (33b)$$

Figure 1 shows a schematic of the domain in the complex $(\phi^2-\mu)$ plane where nonreal eigenvalues are allowed. Only the upper half plane is plotted. The domain is symmetric relative to the real axis. When h_- is zero, the inner curve shrinks to the origin.

Further information about the location of the eigenvalues, which was previously obtained by Moore,[12] can be obtained by taking the real part of Eq. (29). Using the negativity of the first term in that equation we then find that

$$\int_{-\infty}^{\infty} d\bar{y} \, |\delta E_x|^2 \left[\mathrm{Re}(\phi^2) - \frac{\alpha \bar{h} \{ [\mathrm{Re}(\phi^2-\mu)]^2 - [\mathrm{Im}(\phi^2)]^2 \}}{|\phi^2-\mu|^4} \right] > 0 . \quad (34)$$

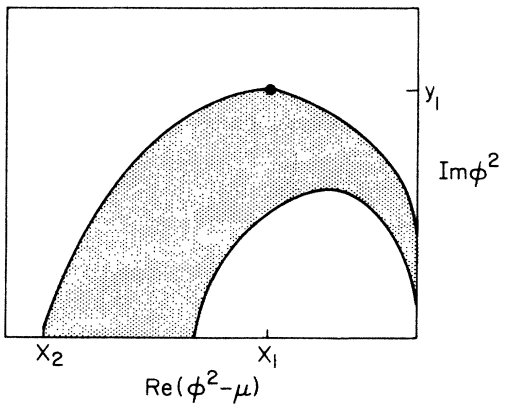

FIG. 1. The domain in the complex $(\phi^2-\mu)$ plane where nonreal eigenvalues are allowed.

We multiply Eq. (30) by $\mathrm{Re}(\phi^2)$, subtract it from Eq. (34), and obtain

$$\mathrm{Im}(\phi^2) > 3[\mathrm{Re}(\phi^2-\mu)]^2 + 2\mu \mathrm{Re}(\phi^2-\mu) . \quad (35)$$

Thus nonreal eigenvalues are allowed in the part of the complex $(\phi^2-\mu)$ plane which is bounded from below by the parabola described by Eq. (35). When the parabola crosses the real axis at a point larger than X_2 only a part of the domain shown in Fig. 1 is allowed. In particular, when $\mu \to -\infty$ only a small part of that domain, the part very close to the imaginary axis, remains allowed. On the other hand, if

$$\frac{-2\mu}{3} < X_2 , \quad (36)$$

the nonreal eigenvalues have to be sought in the whole

domain shown in Fig. 1.

Before we turn to the solution of Eq. (24) for two specific density profiles, we formulate an equivalent problem which is defined for $\bar{y}$ on $[0,\infty)$, instead of for $\bar{y}$ on $(-\infty,\infty)$. We limit ourselves to electron beams of symmetric density

$$\bar{h}(\bar{y})=\bar{h}(-\bar{y}) . \tag{37}$$

The problem we solve is a two-point boundary value problem in which

$$\delta E_x(\pm L)=0 , \tag{38}$$

where L equals 1 when conductors are located at the boundaries of the electron beam and at infinity in the absence of a waveguide. Because of the symmetry of both the density (37) and the boundary conditions (38), Eq. (24) has two families of solutions, symmetric and antisymmetric with respect to $\bar{y}$. Therefore, it is sufficient to solve Eq. (24) for $\bar{y}\geq 0$, where the boundary conditions are

$$\delta E_x'(0)=0=\delta E_x(L) \tag{39}$$

for the symmetric solutions, and

$$\delta E_x(0)=0=\delta E_x(L) \tag{40}$$

for the antisymmetric solutions. In Secs. IV and V we solve Eq. (24) with the boundary conditions (39) for two density profiles.

IV. AN ELECTRON BEAM OF CONSTANT DENSITY

A. The density profile

We start with a uniform electron beam of density

$$\bar{h}(\bar{y})=\begin{cases}1, & |\bar{y}|\leq 1\\ 0, & |\bar{y}|\geq 1 .\end{cases} \tag{41}$$

The symmetric solution inside the beam is

$$\delta E_x=e^{-i\chi\bar{y}}+e^{i\chi\bar{y}},\quad \bar{y}<1 \tag{42}$$

where

$$\chi^2=\phi^2-\frac{\alpha}{(\phi^2-\mu)^2} . \tag{43}$$

B. Guided waves

In the case of guided waves, when a conductor is located at $\bar{y}=\pm 1$, the quantities h_+ and h_- are equal, and the domain of allowed nonreal eigenvalues shrinks to a curve. The boundary conditions specify a discrete set of eigenvalues. The boundary condition at $\bar{y}=1$ yields

$$e^{-i\chi}+e^{i\chi}=0 , \tag{44}$$

and thus

$$\chi_n^2=\left[\frac{\pi}{2}\right]^2(2n+1)^2\quad (n=0,1,2,\ldots) . \tag{45}$$

From the definition (43) we get

$$\phi_n^2-\frac{\alpha}{(\phi_n^2-\mu)^2}=\left[\frac{\pi}{2}\right]^2(2n+1)^2 , \tag{46}$$

which may also be written as

$$(\phi_n^2-\mu)^2\left[\phi_n^2-\left[\frac{\pi}{2}\right]^2(2n+1)^2\right]-\alpha=0 . \tag{47}$$

Equation (47) is a cubic polynomial for ϕ_n^2 of the form similar to that in the 1D theory of the FEL. For every n, if the mismatch parameter satisfies

$$\mu=\left[\frac{\pi}{2}\right]^2(2n+1)^2 , \tag{48}$$

ϕ_n^2 has a maximal imaginary part

$$\mathrm{Im}\phi_n^2=\frac{\sqrt{3}}{2}\alpha^{1/3} . \tag{49}$$

Thus the various eigenmodes have the same maximal growth rate. For large n, Eq. (46) ceases to be valid, since χ_n becomes large and the approximation we used ($\omega\cong k$) no longer holds true. The polynomial (46) has, for any n, three roots which correspond to three modes. When

$$\mu\ll\left[\frac{\pi}{2}\right]^2(2n+1)^2 \tag{50}$$

is satisfied, the modes are nonresonant. One root is then large and real,

$$\phi_n^2\cong\left[\frac{\pi}{2}\right]^2(2n+1)^2 \tag{51}$$

and is close to the vacuum waveguide eigenvalue. The other two roots are close to μ and satisfy

$$-\frac{\alpha}{(\phi_n^2-\mu)^2}\cong\left[\frac{\pi}{2}\right]^2(2n+1)^2 . \tag{52}$$

In Fig. 1, ϕ_n^2 of Eq. (52), for $n\to\infty$, tend to the origin along the curve in the upper half-plane and are nearly pure imaginary. They are

$$\phi_n^2-\mu=\pm\frac{2\alpha^{1/2}i}{(2n+1)\pi} . \tag{53}$$

Thus, $\phi^2=\mu$ is an accumulation point of a series of eigenvalues which correspond to nonresonant unstable modes.

C. Unbounded waves

We now turn to the case of unbounded waves. The solution outside the beam which vanishes at infinity is

$$\delta E_x=be^{i\phi\bar{y}},\quad \bar{y}>1,\quad \mathrm{Im}\phi>0 . \tag{54}$$

We require the field and its derivative to be continuous at the beam boundary, and thus

$$e^{i\chi}+e^{-i\chi}=be^{i\phi} , \tag{55a}$$

$$\chi(e^{i\chi}-e^{-i\chi})=\phi be^{i\phi} . \tag{55b}$$

Equations (43), (55a), and (55b) determine ϕ, χ, and b. By dividing the two last equations we obtain the dispersion relation

$$\frac{\chi(e^{i\chi}-e^{-i\chi})}{(e^{i\chi}+e^{-i\chi})}=\phi \ . \tag{56}$$

The domain of allowed nonreal eigenvalues is again seen in Fig. 1, where the inner bounding curve shrinks to the origin. One could search numerically for the eigenvalues ϕ^2 in that domain. However, for large and small α's, it is possible to derive analytic approximations for the eigenvalues with the largest imaginary part.

We start with large α. We expect ϕ to be much larger than χ, and from Eq. (56) we approximate

$$e^{i\chi}+e^{-i\chi}=0 \ . \tag{57}$$

The wave at the beam boundary is very small but the wave derivative is not that small. To lowest order, χ is

$$\chi_0=(2n+1)\frac{\pi}{2} \tag{58}$$

and the eigenvalue is

$$\phi_0^2\cong\exp(\tfrac{2}{3}i\pi)\alpha^{1/3} \ . \tag{59}$$

Thus, to lowest order, when α is large the eigenvalue is the same as in the 1D theory. The wave profile inside the beam is the same as in the case of a guided wave. The wave is almost confined to the electron-beam volume. This is the case of strong optical guiding.

In order to obtain the form of the wave outside the electron beam we have to solve the equations to the next order. Since χ_0 is $\theta(1)$, we assume χ_1 to be much smaller than 1, and Eq. (56), to first order, becomes

$$\chi_0=i\phi_0\chi_1 \ . \tag{60}$$

This relation enables us to write Eq. (55a), to lowest order, as

$$i\chi_1(e^{i\chi_0}-e^{-i\chi_0})=b_0e^{i\phi_0} \ , \tag{61}$$

which yields

$$b_0=\frac{(2n+1)\pi}{\alpha^{1/6}}\exp\left[i\left[\frac{\pi}{6}-\phi_0\right]\right] \ . \tag{62}$$

For large α the wave is

$$\delta E_x(\bar{y})=\begin{cases}2\cos\left[\left[\frac{\pi}{2}\right](2n+1)\left[1-\frac{(\sqrt{3}+i)}{2\alpha^{1/6}}\right]\bar{y}\right], & \bar{y}\le 1 \qquad (63a)\\ \frac{(2n+1)\pi}{\alpha^{1/6}}\exp\left[i\pi/6+(-i+\sqrt{3})\frac{\alpha^{1/6}}{2}(1-\bar{y})\right], & \bar{y}\ge 1 \ . \qquad (63b)\end{cases}$$

We turn now to the case of small α. The eigenvalue ϕ^2 is then expected to be small, much smaller than χ^2. From the dispersion relation (56) we deduce that, to lowest order,

$$e^{i\chi}-e^{-i\chi}=0 \ , \tag{64}$$

and thus

$$\chi_{n,0}=n\pi \quad (n=0,1,2,3\ldots) \ . \tag{65}$$

We approximate Eq. (43) as

$$\chi^2=-\frac{\alpha}{(\phi^2-\mu)^2} \ , \tag{66}$$

and the eigenvalue becomes, for n larger than zero,

$$\phi^2=\mu+\frac{i\alpha^{1/2}}{n\pi} \quad (n=1,2,\ldots) \ . \tag{67}$$

Larger gain is obtained for the lowest mode ($n=0$). Since χ is much smaller than 1, Eq. (56) becomes

$$i\chi^2=\phi \ . \tag{68}$$

Note that ϕ is indeed much smaller than χ, which is consistent with our assumption. From Eqs. (66) and (68) we obtain

$$i\phi(\phi^2-\mu)^2=\alpha \ , \tag{69}$$

and at resonance, when μ is zero,

$$\phi^2=\alpha^{2/5}e^{3\pi i/5} \ . \tag{70}$$

The eigenvalue of the fundamental mode ($n=0$) has a larger imaginary part than the eigenvalues of the higher modes [Eq. (67)] and thus also a higher gain. As expected, for small α, when diffraction is large, the gain for all modes is lower than in the 1D theory where it scales as $\alpha^{1/3}$. Following Moore[3] we define a normalized gain. Since the eigenvalue ϕ^2 is proportional to a^2 [Eq. (26)], and since the parameter α is proportional to a^5 [Eq. (28)], the normalized gain is defined as

$$g=\mathrm{Im}(\phi^2)/\alpha^{2/5} \ . \tag{71}$$

Using Eqs. (59) and (70) we may now write the normalized gains for large and small α's. They are

$$g=\begin{cases}\frac{\sqrt{3}}{2}\alpha^{-1/15} & \text{as } \alpha\to\infty \qquad (72a)\\ \sin(\frac{3}{5}\pi) & \text{as } \alpha\to 0 \ . \qquad (72b)\end{cases}$$

Note that the result here for the rectangular beam is different from the result for the cylindrical beam.[3] For small α's, the normalized gain for the rectangular beam converges to a constant while it diverges for the cylindrical beam.

We now write the explicit form of the transverse wave profile for small α's. At resonance for the fundamental mode

$$\chi = e^{-i\pi/10}\alpha^{1/10} \tag{73}$$

and thus when α is small,

$$\delta E_x = \begin{cases} 1+\exp(\frac{4}{5}i\pi)\alpha^{1/5}\dfrac{\bar{y}^2}{2}, & \bar{y}\le 1 \quad (74a) \\ [1-\exp(\frac{4}{5}i\pi)\alpha^{1/5}/2]\exp[\exp(\frac{4}{5}i\pi)\alpha^{1/5}\bar{y}], & \bar{y}>1 \ . \quad (74b) \end{cases}$$

This completes the analysis of the FEL which employs a constant density electron beam. In Sec. V we turn to the case of a nonuniform electron beam.

V. AN ELECTRON BEAM OF NONCONSTANT DENSITY

A. General analysis

We study the FEL which employs an electron beam of the following, relatively simple, density profile:

$$\bar{h}(\bar{y}) = \begin{cases} 2(1-|\bar{y}|), & |\bar{y}|\le 1 \quad (75a) \\ 0, & |\bar{y}|\ge 1 \ . \quad (75b) \end{cases}$$

The two density profiles are shown in Fig. 2. We limit ourselves to the symmetric solutions and solve for positive $\bar{y}$ only. Since h_- is zero here the inner curve in Fig. 1 shrinks to the origin. The domain in the complex plane where nonreal eigenvalues are allowed is therefore the same for both guided waves and unbounded waves. Equation (24) becomes

$$\frac{\partial^2\delta E_x}{\partial\bar{y}^2}+\left[\phi^2-\frac{2\alpha(1-\bar{y})}{(\phi^2-\mu)^2}\right]\delta E_x=0, \quad 0\le\bar{y}\le 1 \ . \tag{76}$$

We define a new independent variable ζ,

$$\bar{y}=p\zeta+q \ , \tag{77}$$

where

$$p=-\left[\frac{(\phi^2-\mu)^2}{2\alpha}\right]^{1/3} \tag{78}$$

and

$$q=1-\frac{\phi^2(\phi^2-\mu)^2}{2\alpha} \ , \tag{79}$$

and write Eq. (76) as

$$\frac{\partial^2\delta E_x}{\partial\zeta^2}-\zeta\delta E_x=0 \ . \tag{80}$$

This is Airy's equation, and its general solution is[13]

$$\delta E_x = a_1 A_i(\zeta)+b_1 B_i(\zeta) \ . \tag{81}$$

We are interested in the solution on the semi-infinite line in the complex ζ plane which starts at $\zeta=\zeta_0$ and passes through $\zeta=\zeta_1$, where

$$\zeta_0=-q/p, \quad \zeta_1=(1-q)/p \ . \tag{82}$$

Since we limit ourselves to the symmetric solution, we require as a first boundary condition, that the derivative vanish at ζ_0:

$$a_1 A_i'(\zeta_0)+b_1 B_i'(\zeta_0)=0 \ . \tag{83}$$

We start by studying guided waves and then turn to unbounded waves.

B. Guided waves

When a conductor is located at the beam edge, there is a second boundary condition:

$$a_1 A_i(\xi_1)+b_1 B_i(\zeta_1)=0 \ . \tag{84}$$

Equations (83) and (84) for a_1 and b_1 have nontrivial solutions if their determinant is zero. The dispersion relation is thus

$$A_i'(\zeta_0)B_i(\zeta_1)-B_i'(\zeta_0)A_i(\zeta_1)=0 \ . \tag{85}$$

The eigenvalues can be found by searching numerically in the domain in Fig. 1. We do not solve Eq. (85), but show that, as in the case of constant density, the origin in the complex $\phi^2-\mu$ plane is an accumulation point of nonreal eigenvalues along a curve close to the imaginary axis.

When ϕ^2 is close to μ, q is nearly 1, and p is very large. Then ζ_1 is close to zero, and ζ_0 is very large. The dispersion relation (85) is approximately

$$\frac{B_i'(\zeta_0)}{A_i'(\zeta_0)}=\frac{B_i(0)}{A_i(0)}=\sqrt{3} \ . \tag{86}$$

We use the asymptotic expressions for the Airy functions, assume that the argument of ζ_0 is smaller than $\pi/3$, and obtain

$$-2\exp(\tfrac{2}{3}\zeta_0^{3/2})=\sqrt{3} \ . \tag{87}$$

For large n we find ζ_0 to be

$$\zeta_0=[\tfrac{3}{2}(2n+1)\pi i]^{2/3}\left[1+\frac{2}{3}\frac{\ln(\sqrt{3}/2)}{(2n+1)\pi i}\right] \ . \tag{88}$$

The argument of ζ_0 is close to but smaller than $\pi/3$, consistent with our assumption. From the definition of ζ_0 [Eq. (82)], we see that for each n two of the eigenvalues ϕ_n^2 are nonreal and satisfy approximately

$$\phi_n^2-\mu=\pm\frac{2}{3}\frac{(2\alpha)^{1/2}i}{(2n+1)\pi} \ . \tag{89}$$

Thus, as in the constant density case (53), $\phi^2=\mu$ is an accumulation point of a series of eigenvalues which correspond to nonresonant unstable modes. We now turn to the case of unbounded waves.

C. Unbounded waves

The wave outside the beam has the same form for both constant and nonconstant densities:

$$\delta E_x = Ce^{i\phi\bar{y}}, \quad \bar{y} > 1 \ . \tag{90}$$

We require the field and its derivative to be continuous at $\bar{y}=1$,

$$a_1 A_i(\zeta_1) + b_1 B_i(\zeta_1) = Ce^{i\phi} \ , \tag{91a}$$

$$\frac{1}{p}[a_1 A_i'(\zeta_1) + b_1 B_i'(\zeta_1)] = i\phi C e^{i\phi} \ . \tag{91b}$$

Equations (83), (91a), and (91b) have nontrivial solutions for a_1, b_1, and C if

$$\left[\frac{B_i'(\zeta_0)A_i'(\zeta_1) - A_i'(\zeta_0)B_i'(\zeta_1)}{B_i'(\zeta_0)A_i(\zeta_1) - A_i'(\zeta_0)B_i(\zeta_1)}\right] = \zeta_1^{1/2} \ , \tag{92}$$

where $i\phi p$ equals $\zeta_1^{1/2}$. Equation (92) is the dispersion relation for unbounded waves. Numerical examples will be given later. Here we find the eigenvalues analytically for large and small α's.

We start with large α's and study the case of resonance when μ is zero. From the analysis in Sec. III, we know that the largest allowed imaginary part is that of the eigenvalue for which q is zero. We look, therefore, for an eigenvalue for which q goes to zero when α is large. For such an eigenvalue, ζ_1 obeys

$$\zeta_1 \rightarrow |2\alpha|^{1/9}\exp(\tfrac{5}{9}i\pi) \ , \tag{93}$$

as $\alpha \rightarrow \infty$. We look for eigenvalues which have large imaginary parts such that ζ_0 is $\theta(1)$. Substituting the asymptotic form of Airy's functions and their derivatives[13] into Eq. (92) we see that some of the terms in the equation are proportional to $\exp(-\frac{2}{3}\zeta_1^{3/2})$ which diverges for large α. The rest of the terms are proportional to $\exp(\frac{2}{3}\zeta_1^{3/2})$ which decays for large α and, to lowest order, joins smoothly the solution outside the beam. Equation (92) is thus replaced by the requirement that the coefficient of $\exp(-\frac{2}{3}\zeta_1^{3/2})$ is zero. To lowest order in $1/\zeta_1$, we obtain

$$-B_i'(\zeta_0) - \frac{A_i'(\zeta_0)}{i}e^{i\pi/4} = B_i'(\zeta_0) - A_i'(\zeta_0)e^{i\pi/4} \ . \tag{94}$$

We find ζ_0 numerically:

$$\zeta_0 = \eta = 0.48 - i1.26 \ . \tag{95}$$

The eigenvalue is thus, asymptotically,

$$\phi^2 = (2\alpha)^{1/3}\exp(\tfrac{2}{3}i\pi)\left[1 - \frac{\eta}{3}(2\alpha)^{-1/9}\exp(\tfrac{4}{9}i\pi)\right] \ . \tag{96}$$

The asymptotic solution for large α, not too close to the origin, is

$$\delta E_x = \begin{cases} \exp[\frac{2}{3}(2\alpha)^{1/6}e^{5\pi i/6}\bar{y}^{3/2}] \ , \\ \qquad\qquad (2\alpha)^{-1/9} \ll \bar{y} \le 1 & \text{(97a)} \\ \exp[(2\alpha)^{1/6}e^{5\pi i/6}(\bar{y} - \frac{1}{3})] \ , \\ \qquad\qquad \bar{y} \ge 1 \ . & \text{(97b)} \end{cases}$$

It is difficult to compute the wave profile for large α's by matching a numerical solution of the differential equation inside the beam to a solution for $\bar{y}$ greater than 1 (outside the beam), since for most values of ϕ^2 the solutions diverge near the beam boundary. Instead, one should seek a solution which joins smoothly the function in (97a) for $\bar{y}$ several times greater than $(2\alpha)^{-1/9}$ but still much smaller than 1.

We now turn to the solution for small α's. We assume that ζ_1 and ζ_0 are small and expand the Airy's functions in their small arguments. The dispersion equation (92) becomes

$$\frac{-\zeta_0^2}{2} = \zeta_1^{1/2} \ . \tag{98}$$

Since q [Eq. (79)] is nearly 1, we obtain the following equation for the eigenvalue:

$$\frac{\phi^2(\phi^2-\mu)^2}{2\alpha} = -\frac{2\alpha}{4(\phi^2-\mu)^2} \ . \tag{99}$$

At resonance, the eigenvalue with the maximum imaginary part is

$$\phi^2 = \alpha^{2/5}e^{3\pi i/5} \ , \tag{100}$$

and the normalized gain (71) is

$$g = 2^{1/3}\frac{\sqrt{3}}{2}\alpha^{-1/15}, \quad \alpha \rightarrow \infty \tag{101a}$$

and

$$g = \sin(3\pi/5), \quad \alpha \rightarrow 0 \ . \tag{101b}$$

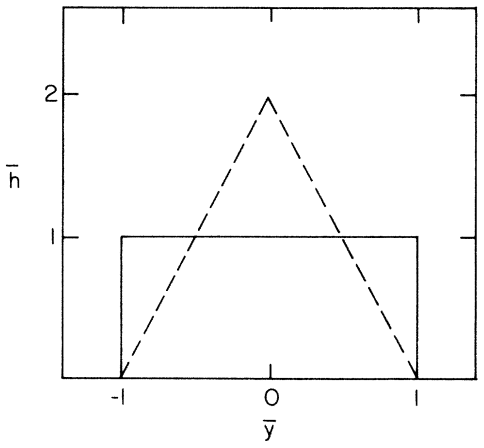

FIG. 2. The two density profiles: The constant density beam (solid line) and the triangular-shaped beam (dashed line).

For small α's the wave field is

$$\delta E_x = \begin{cases} 1+\alpha^{1/5}\exp(\frac{4}{5}i\pi)[\bar{y}-\frac{1}{3}(\bar{y}-1)^3], & \bar{y}\le 1 \\ \exp[\alpha^{1/5}\exp(\frac{4}{5}i\pi)\bar{y}], & \bar{y}\ge 1 \ . \end{cases} \quad (102)$$

Comparing the two density profiles, we see that for large α's, the gain of a FEL which employs the nonconstant density beam [Eq. (96)] is larger by a factor of $2^{1/3}$ than the gain of a FEL which employs a constant density beam [Eq. (59)]. For small α's, however, the gain is the same for both density profiles [Eqs. (70) and (100)]. For the large diffraction case, i.e., small α, the eigenvalue of the fundamental mode is not sensitive to the density profile of the electron beam. When α is large and optical guiding is strong, the gain is proportional to $\alpha^{1/3}$, as in the 1D theory. When α is small and diffraction is large, the electron beam occupies only a small part of the volume occupied by the wave. The interaction is then weaker and the gain scales as $\alpha^{2/5}$

VI. NUMERICAL SOLUTIONS AND DISCUSSION

In this section we present the calculated wave transverse profiles for various values of α for the two density profiles. We also show the normalized gain as a function of α. All the examples refer to the fundamental mode and to the case of resonance ($\mu=0$).

In Figs. 3–5 the solid line describes the wave profiles for the constant density profile, while the dashed line shows the wave profiles for the triangular-shaped density profile. The wave magnetic field δB_z is simply the y derivative of δE_x. The vertical units are arbitrary; it is the relative intensity that is important. The plots show the absolute values of the electric and the magnetic fields.

In Fig. 3 we show the wave profiles for the case of strong optical guiding. For a large coupling parameter ($\alpha=0.5\times10^9$) the absolute values of the wave electric field [Fig. 3(a)] and of the wave magnetic field [3(b)] are shown. For the beam of constant density the wave extends to $\bar{y}$ equals 1 and then decreases abruptly. The derivative of the magnetic field is not continuous at $\bar{y}$ equals 1 since the current is not continuous there for this density profile. For the triangular-shaped beam the wave

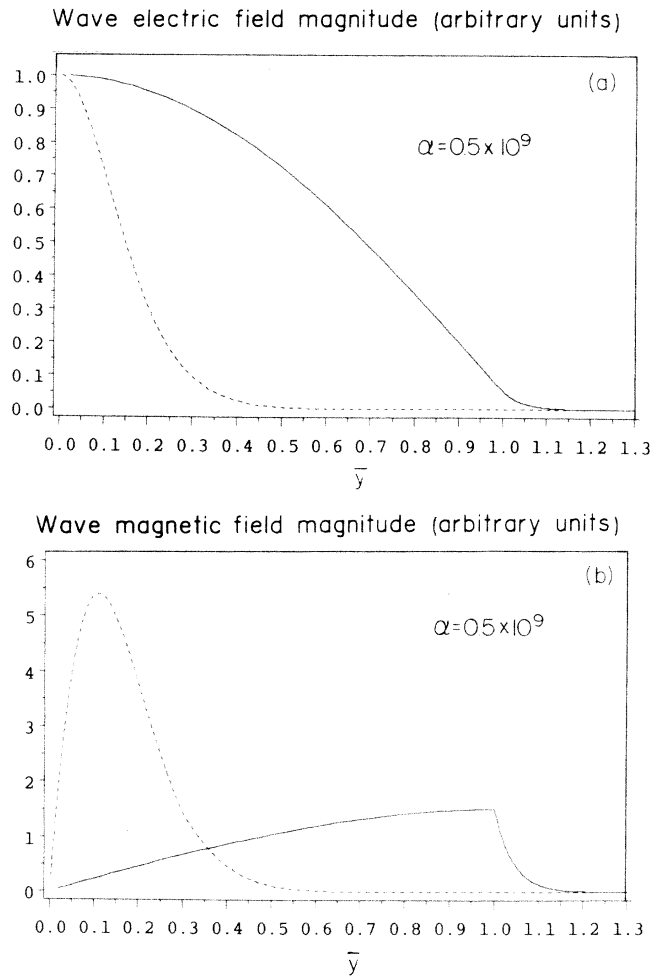

FIG. 3. The absolute value of (a) the wave electric field and (b) the wave magnetic field for $\alpha=0.5\times10^9$ and $\mu=0$, for the constant density beam (solid line) and for the triangular-shaped beam (dashed line).

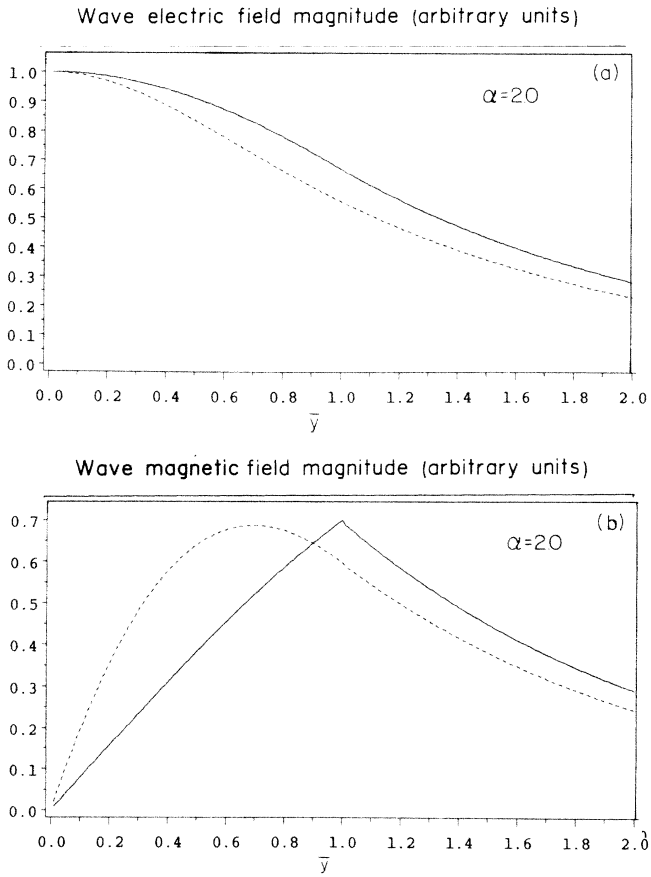

FIG. 4. The absolute value of (a) the wave electric field and (b) the wave magnetic field for $\alpha=2$ and $\mu=0$ for the constant density beam (solid line) and for the triangular-shaped beam (dashed line).

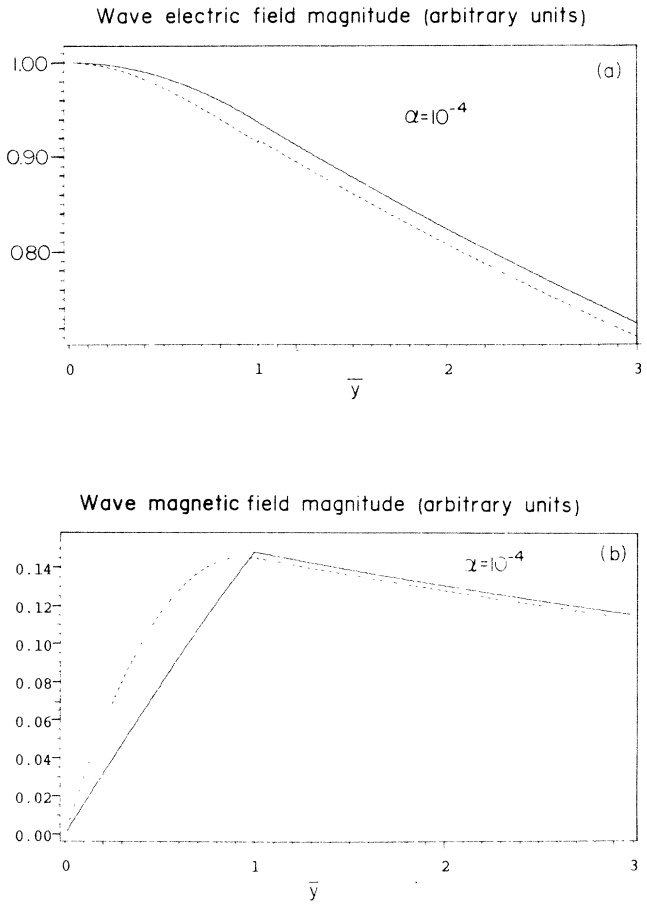

FIG. 5. The absolute value of (a) the wave electric field and (b) the wave magnetic field for $\alpha=10^{-4}$ and $\mu=0$, for the constant density beam (solid line) and for the triangular-shaped beam (dashed line).

is localized near the midplane ($\bar{y}=0$) and decays to nearly zero inside the electron beam volume. While for the constant density beam the wave profile converges to a shape given by Eq. (63) when α is infinity, for the triangular-shaped beam the wave tends to be confined more and more to the midplane, and its thickness tends to zero. For the computation of the wave profile for the constant density beam we employed Eq. (63). For the triangular-shaped beam we employed the numerical procedure described in Sec. V. The solution of the differential equation and its derivative were required at $\bar{y}=0.3$ [which is three times $(2\alpha)^{-1/9}$] to equal the values of the function (97a) and its derivative. The computed eigenvalue ϕ^2 is $-473.56+i844.05$.

Figures 4(a) and 4(b) show the wave profiles for α equal 2. The wave for the constant density beam occupies a larger volume than the wave for the triangular-shaped beam. The eigenvalue ϕ^2 is $-0.438+i0.978$ for the constant density beam and $-0.438+i1.046$ for the triangular-shaped beam.

Figures 5(a) and 5(b) show the wave profiles for the case of large diffraction, when α is 10^{-4}. The eigenvalues are nearly identical for the two density profiles, and the wave profiles are also similar. The wave profile for the constant density beam was found according to Eq. (74) and for the triangular-shaped beam according to Eq. (102).

Figure 6 shows the normalized gain g [Eq. (71)] versus $\log_{10}\alpha$ for the two density profiles. The curve with larger g shows the gain for the triangular-shaped beam. The gain was found by solving the differential equation (24) numerically and by looking for ϕ^2 with the largest imaginary part for which the boundary conditions are satisfied. These results are denoted in Fig. 6 by solid lines. The results for large α's are denoted by dashed lines. For large α's the gain was calculated by Eq. (72) for the constant density beam and by Eq. (101a) for the triangular-shaped beam. The two parts of each curve join smoothly. For small α's the normalized gain converges to a limiting value, identical for both density profiles [Eqs. (72b) and (101b)].

Thus when optical guiding is strong, the gain for the triangular-shaped beam is larger by a factor of $2^{1/3}$ than for the constant density beam. When diffraction is large, however, the results are not sensitive to the density profile, and the gain is the same for both density profiles.

When the current J is kept constant, the dependence of the gain on the beam thickness a is expressed through the dependence of the normalized gain g on $\alpha^{1/5}$. In this case the gain is increased by reducing the beam thickness and thus increasing the beam density. The dependence of the normalized gain on α demonstrates this feature. However, the decrease in the beam thickness is followed by an increase in the diffraction and a decrease in the filling factor, and this decrease has the opposite effect of reducing the gain. These two contradictory effects cancel each other out and the gain for small thickness has an upper bound. One should note that such an upper bound for the gain does not exist for a cylindrical beam[3] where the

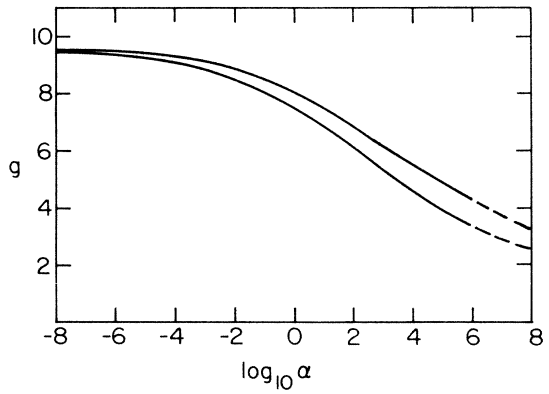

FIG. 6. The normalized gain vs $\log_{10}\alpha$ for the two density profiles. The upper curve shows the gain for the triangular-shaped beam and the lower curve the gain for the constant density beam.

gain goes to infinity (albeit very slowly) when the radius of the beam goes to zero.

When the beam thickness is constant, the dependence of the gain on the current is expressed through the dependence of $\mathrm{Im}\phi^2$ on α. In this case the gain grows when the current grows.

ACKNOWLEDGMENTS

Useful discussions with Mr. Eli Jerby, Dr. Michael Magen, and Dr. Ilan Ben-Zvi are acknowledged. The author acknowledges financial support by the Sir Charles Clore Foundation.

[1]T. C. Marshall, *Free Electron Lasers* (Macmillan, New York, 1985), and references therein.

[2]E. T. Scharlemann, A. M. Sessler, and J. S. Wurtele, Phys. Rev. Lett. **54**, 1925 (1985).

[3]G. T. Moore, Nucl. Instrum. Methods **A239**, 19 (1985).

[4]Proceedings of the Eighth International Free Electron Laser Conference, Glasgow, U.K., 1986, edited by M. W. Poole [Nucl. Instrum. Methods **A259**, 136 (1987)].

[5]P. Sprangle, A. Ting, and C. M. Tang, Phys. Rev. Lett. **59**, 202 (1987).

[6]J. Fajans and G. Bekefi, Phys. Fluids **29**, 3461 (1986).

[7]V. L. Granatstein, Ninth International Free Electron Laser Conference, Williamsburg, Virginia, 1987 (unpublished).

[8]H. Weitzner, A. Fruchtman, and P. Amendt, Phys. Fluids **30**, 539 (1987).

[9]A. Fruchtman, Phys. Fluids **30**, 2496 (1987).

[10]A. Fruchtman, Phys. Rev. A (to be published).

[11]P. G. Drazin and W. H. Reid, *Hydrodynamic Stability* (Cambridge University Press, Cambridge, 1984), p. 131.

[12]G. T. Moore (unpublished).

[13]*Handbook of Mathematical Functions,* edited by M. Ambramowitz and I. A. Stegun (Dover, New York, 1972), p. 446.

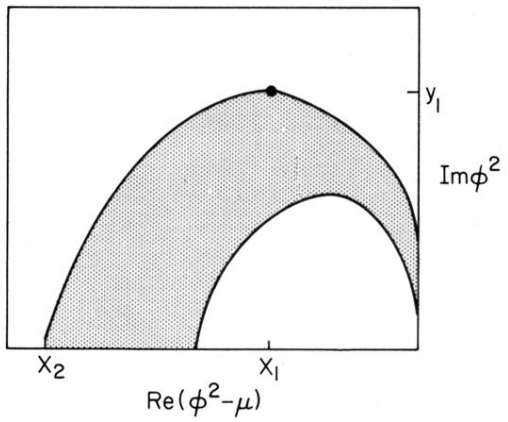

FIG. 1. The domain in the complex $(\phi^2-\mu)$ plane where nonreal eigenvalues are allowed.